ISSN 1070-3284, Russian Journal of Coordination Chemistry, 2016, Vol. 42, No. 9, pp. 557–573. © Pleiades Publishing, Ltd., 2016.
Original Russian Text © D.N. Dybtsev, D.G. Samsonenko, V.P. Fedin, 2016, published in Koordinatsionnaya Khimiya, 2016, Vol. 42, No. 9, pp. 515–531.

Porous Coordination Polymers Based on Carboxylate Complexes of 3*d* Metals

D. N. Dybtsev, D. G. Samsonenko, and V. P. Fedin*

Nikolaev Institute of Inorganic Chemistry, Siberian Branch, Russian Academy of Sciences, pr. akademika Lavrentieva 3, Novosibirsk, 630090 Russia

**e-mail: cluster@niic.nsc.ru*

Received February 3, 2016

Abstract—The results of our studies on the synthesis of porous metal-organic coordination polymers (including homochiral frameworks) based on 3*d*-metal cations and bridges of two types (carboxylate and N-donor ligands) and investigations of their sorption and catalytic properties are summarized in the review.

Keywords: porous coordination polymers, metal-organic frameworks, carboxylates, gas sorption, catalysis, separation of enantiomers

DOI: 10.1134/S1070328416090013

INTRODUCTION

The modern history of coordination polymers starts in 1989 from the pioneer work by Robson [1], who predicted huge prospects of module design for the coordination polymers, i.e., the possibility to join together organic and inorganic building fragments of certain geometry into coordination structures with an identical topology but variable geometric parameters of the framework. The foundations for the purposeful design of coordination metal-organic structures were thus formed [2].

In 1990s, Robson, Zaworotko, Fujita, Yaghi, Prosperio, Kanatzidis, Schröder, et al. prepared a series of crystalline coordination polymers with large channels filled with molecules of guests (solvents). Undoubtedly, N-donor bridging ligands of the type of 4,4'-bipyridine [3–5] or nitrile derivatives [6] predominated in the chemistry of coordination polymers up to 2000. The structures of a significant number of the porous coordination polymers synthesized at the moment were cationic due to the electroneutral character of the bridging ligands. Thus, the anion was an essential part of the free interframework space.

At the same time, attempts to obtain permanently porous coordination frameworks demonstrating reversible gas sorption remained unsuccessful for a long time. The first examples of these compounds were published by Kitagawa in 1997 [7] and Yaghi in 1998 [8]. The sorption characteristics of these frameworks were low. For example, the specific surface area of the compound synthesized by Yaghi was 310 m^2/g, which is typical of the most part of microporous zeolites. A reason for such modest results is, first, the presence of anions in the cavities. Second, the nature of monodentate N-donor ligands assumes more possibilities for the mechanical deformation of the porous framework and its "collapse." The breakthrough in this direction was made on going from monodentate electroneutral bridging ligands to bi- and tridentate ligands (carboxylates and others). This replacement of the ligands made it possible to solve two problems simultaneously. On the one hand, the use of anionic carboxylate ligands compensates a positive charge of the metal cations, providing the formation of electroneutral coordination frameworks, whose cavities have no anions. On the other hand, the presence of polydentate coordinating groups substantially enhances the mechanical strength of the porous coordination frameworks upon the removal of solvent molecules from the cavities. The first coordination polymers $[Cu_2(Btc)_{2/3}(H_2O)_2]$ (HKUST-1) [9] and $[Zn_4O(Bdc)_3]$ (MOF-5) [10] demonstrating outstanding sorption properties, which significantly exceeded those of all porous materials known at the moment, were obtained in 1999 using the carboxylate ligands.

Fundamental problems related to the rational design of coordination structures with specified parameters of the cavities were solved in parallel to the problems on the synthesis of porous coordination polymers and studies of their properties. The module Robson's approach to the synthesis of porous coordination polymers was developed by Férey [11], who considered metal-organic coordination polymers as an evolutional continuation of zeolites, being inor-

ganic coordination polymers. According to the Férey scheme, metal-organic coordination frameworks could be obtained by joining layered inorganic secondary building units through organic bridges in one direction (3D = 2D + 1D), chain units in two directions (3D = 1D + 2 × 1D), or isolated units in three directions (3D = 0D + 3 × 1D).

The use of several organic ligands for the preparation of porous framework structures has both several advantages (for example, the possibilities for fine controlling the framework geometry and functionality of the internal space are substantially extended) and drawbacks. Among the latter are possible impurities formed under non-optimized synthesis conditions and a decrease in rationality of design; i.e., in many cases, it is very difficult to a priori predict the entire or even partial structure of the obtained crystal structure. At the same time, the valid post-synthetic analysis of intermediate results makes it possible to reveal stable building motifs and to perform the purposeful synthesis of the whole families of isoreticular porous coordination structures with varied geometric parameters of the cavities [12–15].

The results of our studies on the synthesis of porous metal-organic coordination polymers (including homochiral structures) based on 3*d*-metal cations and bridges of two types (carboxylate and N-donor ligands) and investigations of their sorption and catalytic properties are summarized in this review.

COMPOUNDS BASED ON BINUCLEAR BUILDING UNITS

Organic compounds with one or several carboxylate groups are convenient and available reagents for the preparation of various coordination polymers. Polynuclear carboxylate and oxocarboxylate complexes with various geometries, whose structures are well known from classical coordination chemistry, namely, $[M_2(RCOO)_4(L)_2]$, $[M_3(RCOO)_6(L)_2]$, $[M_3O(RCOO)_6(L)_3]$, and $[M_4O(RCOO)_6]$ (L is terminal ligand), often act as inorganic building units in these structures. For instance, the known porous coordination polymer MOF-5 [10] is based on the tetranuclear complexes $[Zn_4O(RCOO)_6]$, whereas HKUST-1 [9] is based on binuclear $[Cu_2(RCOO)_4(L)_2]$ also known as "paddle wheel." The geometry of these complexes is specified rather rigidly, which makes it possible to obtain coordination polymers with a high degree of predictability of the structure by joining the complexes through structurally rigid carboxylate bridges. For example, joining binuclear complexes $\{M_2(RCOO)_4\}$ through linear bridges should result with a high probability in the formation of layered square networks.

If assuming that the formation of a binuclear carboxylate complex is the predominant factor compared to the packing effects, then the introducing of a subsidiary bridging ligand should not substantially affect the structure of the complex and, hence, the geometry of the layered motif. The linear bidentate bridges should pull apart and connect the carboxylate layers in the perpendicular direction. In these hierarchic framework structures, the carboxylate layers can be considered as tertiary building units, whose linking through various bridges can purposefully give porous coordination structures with a controlled distance between the layers. We successfully demonstrated an idea of this stage-by-stage design of coordination frameworks based on two different linear ligands for various coordination polymers. The corresponding results are presented in this section.

The use of short dicarboxylate ligands (terephthalate, naphthalenedicarboxylate) and/or the addition of an organic base result in the crystallization of layered coordination structures based on binuclear zinc complexes $[Zn_2(RCOO)_4(L)_2]$. Four carboxylate ligands RCOO form a square around each of two metal cations, and one N-donor ligand L coordinates to each metal atom perpendicularly to the square to form "incomplete octahedra." Connecting these nodes through structurally rigid linear bridges, one can obtain framework coordination polymers with the primitive cubic topology **pcu** (Fig. 1). It is noteworthy that the use of two types of ligands makes it possible to independently vary the parameters of the framework both within the carboxylate layer and between the layers. In addition, the use of substituted ligands makes it possible to introduce various chemical groups (for instance, hydrophobic, polar, aromatic, or even chiral centers) into the coordination framework without violating the general topology of the framework. The dicarboxylate bridges and N-donor ligands used in the synthesis of the coordination frameworks are exemplified in Fig. 2. The list of the obtained porous metal-organic frameworks is presented in Table 1.

Unfortunately, the primitive cubic topology often favors the formation of interpenetrating (intergrown) coordination structures. In all cases where steric hindrances were absent, compounds $[Zn_2(Xdc)_2(L)]$ (H_2Xdc is terephthalic, 2,6-naphthalenedicarboxylic, or 4,4'-biphenyldicarboxylic acid) crystallized as interpenetrating coordination frameworks with the primitive cubic topology. For example, compound $[Zn_2(Bdc)_2(Bipy)]$ has a doubly intergrown framework, whereas $[Zn_2(Ndc)_2(Bipy)]$ (H_2Ndc is 2,6-naphthalenedicarboxylic acid, and Bipy is 4,4'-bipyridine) is already triply intergrown (Fig. 3). Owing to the intergrowth, a significant part of these coordination polymers is nonporous.

An attentive study of the intergrowth structure in the primitive cubic topology allows one to draw several conclusions. For the *n*-fold interpenetration of the framework with the **pcu** topology, each rectangular cell of any sublattice should be passed through by $n - 1$ linking bridges belonging to other sublattices. From

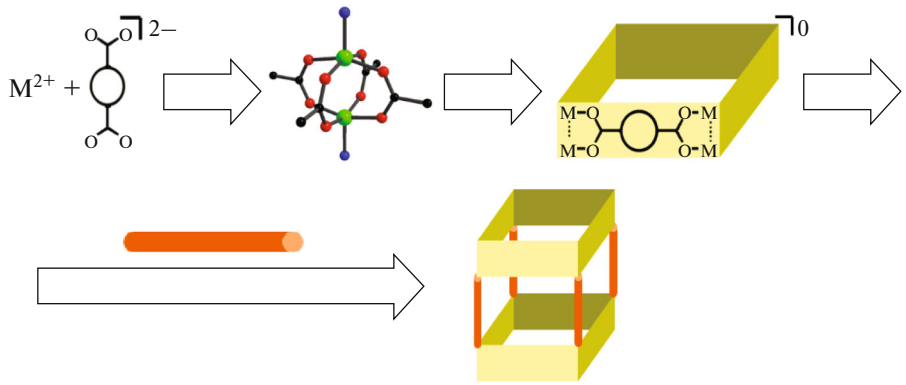

Fig. 1. Formation of the primitive cubic frameworks from the binuclear carboxylate complexes $[M_2(COO)_4]$. The layers with the square geometry of the mesh (**sql**) are linked by the bridging ligands into the **pcu** framework.

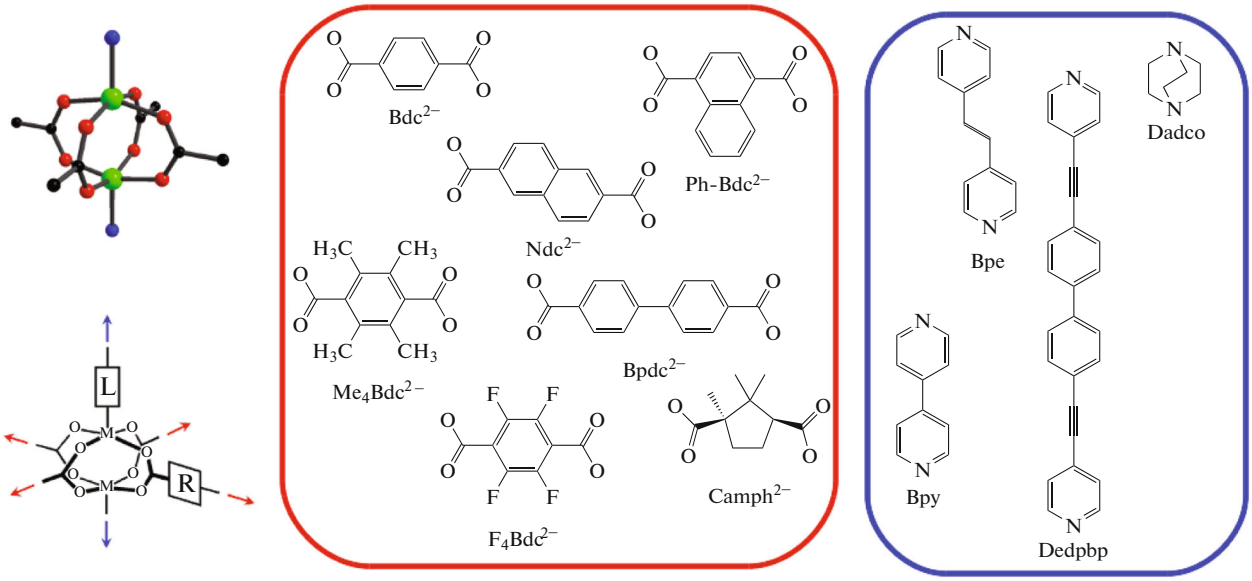

Fig. 2. Representation of the carboxylate complex $[M_2(RCOO)_4(L)_2]$ (at upper left) as an octahedral unit coordinated by ligands of two types (at bottom left); R are the used linear dicarboxylate ligands (at the center); L are the used linear N-donor ligands (on the right).

this it is evident that the maximum degree of interpenetration of the frameworks will be determined by the size of the smallest mesh in the framework. This is consistent with the above example of coordination polymers $[Zn_2(Bdc)_2(Bipy)]$ and $[Zn_2(Ndc)_2(Bipy)]$, since the degree of intergrowth is determined, in this case, by the mesh size in the $\{Zn_2(Xdc)_2\}$ layer characterized by the length of the dicarboxylate bridge. However, two types of ligands are used in structures of the $[Zn_2(Xdc)_2(L)]$ type, which provides an independent control of the mesh sizes in the **pcu** framework in two directions. Only the mesh with a minimum size will restrict the degree of intergrowth. In other words, the elongation of one of the bridging ligands with the retention of the minimum size of another bridge should not increase the degree of intergrowth but should lead to an increase in the free space in the structure. This conclusion was remarkably demonstrated for the frameworks $[Zn_2(Ndc)_2(L)]$, where the length of bridging N-donor ligand L increases in the series Bipy, Bpe (Bpe is 4,4'-bis(pyridineethylene)), Dedpbp (Dedpbp is 4,4'-diethynyl-4",4"'-pyridylbiphenyl) [18]. All the three compounds are characterized by the threefold degree of interpenetration of the frameworks restricted by the sizes of the square mesh in the carboxylate networks $\{Zn_2(Ndc)_2\}$. The simultaneous presence of the longer N-donor ligands between the networks leads to an increase in the free

Table 1. Metal-organic frameworks based on the binuclear carboxylate complexes

Framework	Degree of intergrowth*	Literature
$[Zn_2(Bdc)_2(Dabco)]$	1	[16]
$[Zn_2(Bdc)(Me_4Bdc)(Dabco)]$	1	[17]
$[Zn_2(Me_4Bdc)_2(Dabco)]$	1	[17]
$[Zn_2(Ph\text{-}Bdc)_2(Dabco)]$	1	[17]
$[Zn_2(F_4Bdc)_2(Dabco)]$	1	[17]
$[Zn_2(Bdc)_2(Dabco)]$	1	[17]
$[Zn_2(Bdc)_2(Bipy)]$	2	[17]
$[Zn_2(Me_4Bdc)_2(Bipy)]$	1	[17]
$[Zn_2(Ndc)_2(Bipy)]$	3	[17]
$[Zn_2(Ndc)_2(Bpe)]$	2, 3	[18]
$[Zn_2(Ndc)_2(Dedpbp)]$	3	[18]
$[Zn_2(Camph)_2(Dabco)]$	1	[19]
$[Zn_2(Camph)_2(Bipy)]$	1	[19]
$[Zn_2(Camph)_2(Bpe)]$	1	[19]
$[Cu_2(Camph)_2(Dabco)]$	1	[20]
$[Cu_2(Camph)_2(Bipy)]$	1	[20]
$[Cu_2(Camph)_2(Bpe)]$	1	[20]

* Number of independent frameworks (the degree of intergrowth equal to 1 means the absence of intergrowth).

space between the polymer sublattices. According to the calculations using the PLATON program [21], the accessible free volume in the intergrown metal-organic frameworks $[Zn_2(Ndc)_2(Bipy)]$, $[Zn_2(Ndc)_2(Bpe)]$, and $[Zn_2(Ndc)_2(Dedpbp)]$ is 0, 23, and 43%, respectively.

Using fairly short or sterically substituted bridging ligands, one can completely eliminate intergrowth in such **pcu** structures due to the formation of very small windows through which the ligands cannot penetrate sterically. This rational solution of the problem of intergrowth was successfully demonstrated. For instance, the doubly intergrown metal-organic framework $[Zn_2(Bdc)_2(Bipy)]$ is formed in the Zn^{2+}–H_2Bdc–Bipy system. Intergrowth occurs through the cavities with a size of ~7 × 7 Å in the carboxylate layer $\{Zn_2(Bdc)_2\}$, which is sufficient for the penetration of the Bipy ligands (the cross section of Bipy is ≈6 Å). The use of tetramethylterephthalate (Me_4Bdc^{2-}) results in a partial turn of the benzene rings relative to the carboxylate groups because of the appeared steric repulsion. Owing to this orientation of the substituted benzene rings, the effective size of the window in the $\{Zn_2(Me_4Bdc)_2\}$ layer is only ~3 Å, which is insufficient for intergrowth. As a result, compound $[Zn_2(Me_4Bdc)_2(Bipy)]$ is a non-intergrown primitive cubic framework. Similarly, the use of the short Dabco bridge (Dabco is diazabicyclo[2.2.2]octane) instead of Bipy results in the prohibition of intergrowth.

Chiral dicarboxylic camphor acid (H_2Camph) can also be applied successfully for the preparation of layered structures based on the binuclear fragment $\{M_2(COO)_4\}$. The use of the strategy on connecting layered motifs into a three-dimensional porous framework due to using the additional N-donor ligand L allowed us to obtain for the first time porous homochiral frameworks with varied parameters of the cavities (Table 1). Noteworthy, the intergrowth of metal-organic frameworks in $[Zn_2(Camph)_2(L)]$ is impossible because of the dense structure of the camphorate layer. An interesting difference between $[Zn_2(Camph)_2(Dabco)]$ and $[Zn_2(Camph)_2(Bipy)]$ is the alternating mode of the camphorate layers. In the first structure, the $\{Zn_2(Camph)_2\}$ layers are arranged rigidly above one another (type AAAA), whereas they alternate next nearest in the second structure (type (ABAB, Fig. 4). An attempt to determine the crystal structure of the $[Zn_2(Camph)_2(Bpe)]$ framework using X-ray crystallography was unsuccessful. It can be assumed from the X-ray powder diffraction data that the $\{Zn_2(Camph)_2\}$ layers are joined into the **pcu** framework through the Bpe bridges, and the alternation of the layers relative to each other is irregular.

If ignoring specific features of the layer packing relative to one another in the formation of the $[Zn_2(Camph)_2(L)]$ frameworks, all zinc camphorates can be considered isoreticular. It is more important that the distance between the layered **sql** motifs $\{Zn_2(Camph)_2\}$ are specified by the length of the bridging ligand L and vary from 4.5 Å (Dabco) to 8 Å (Bipy) and 10.5 Å (Bpe) (Fig. 5). Correspondingly, the size of cavities formed in the interlayer space varies. According to the calculations performed using the PLATON program, the volume of the cavities accessible for inclusion in porous camphorates $[Zn_2(Camph)_2(L)]$ is 31, 49, and 55% for L = Dabco, Bipy, and Bpe, respectively. The size of the channels estimated from the structural data is 3 × 3.5 Å for $[Zn_2(Camph)_2(Dabco)]$, 5 × 7 Å for $[Zn_2(Camph)_2(Bipy)]$, and 5 × 10 Å for $[Zn_2(Camph)_2(Bpe)]$.

Porous copper camphorates $[Cu_2(Camph)_2(L)]$ (L = Dabco, Bipy, Bpe) were obtained similarly. Their structural similarity to the corresponding zinc analogs $[Zn_2(Camph)_2(L)]$ was unambiguously concluded on the basis of the X-ray powder diffraction data [20].

POROUS HOMOCHIRAL METAL-ORGANIC FRAMEWORKS

Homochiral coordination structures represent an important class of porous metal-organic frameworks. Since their pores contain asymmetric centers, the

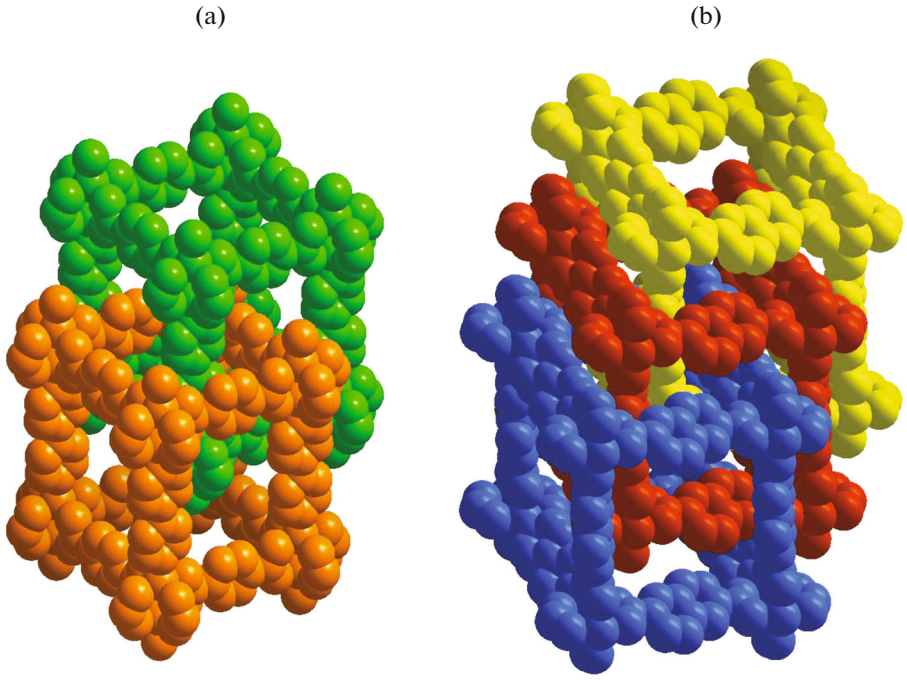

Fig. 3. Crystal structures of (a) $[Zn_2(Bdc)_2(Bipy)]$ and (b) $[Zn_2(Ndc)_2(Bipy)]$ indicating the twofold and threefold intergrowth of the **pcu** frameworks.

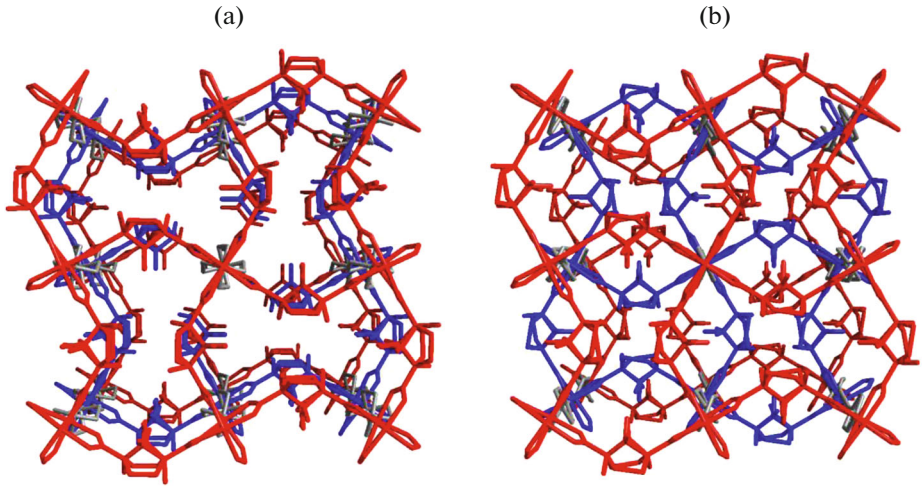

Fig. 4. Packing of the camphorate layers in the structures of (a) $[Zn_2(Camph)_2(Dabco)]$ and (b) $[Zn_2(Camph)_2(Bipy)]$.

affinity of the frameworks to optically active molecules can be changed due to different interactions of guests with chiral hosts, which is a basis for steroselective catalysis. This also allows one to sorb various enantiomers with different selectivities, which is used for steroselective purification and for the separation of chiral antipodes. It is especially important to obtain families of porous structures with finely varied geometric parameters (size and shape of cavities, structure of the chiral center), since this makes it possible to tune the framework to a specific substrate in order to achieve the maximum efficiency of separation and/or catalysis.

The module hierarchic approach to the design of coordination polymers, which has first been advanced by Robson and supplemented by Férey, was additionally developed and successfully used for the preparation of families of enantiopure (homochiral) metal-

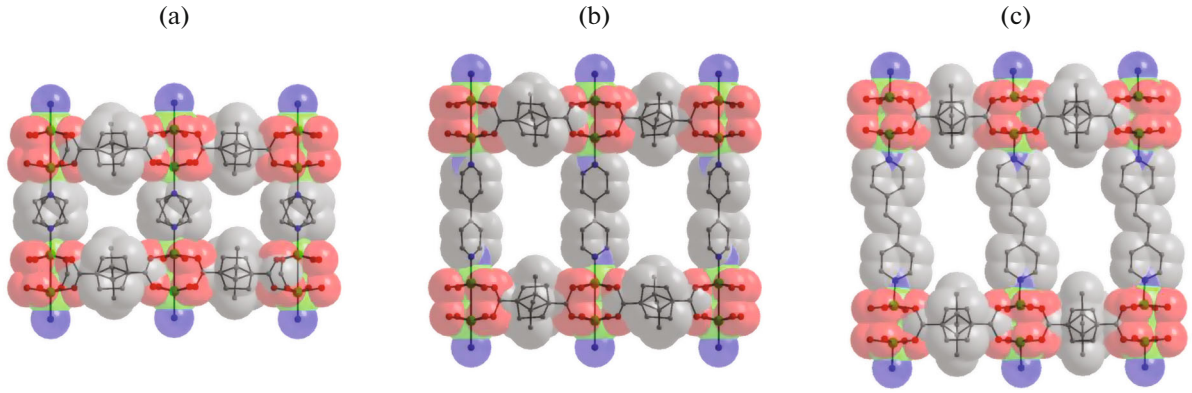

Fig. 5. Porous channels in zinc camphorates $[Zn_2(Camph)_2(L)]$ (L = (a) Dabco, (b) Bipy, and (c) Bpe).

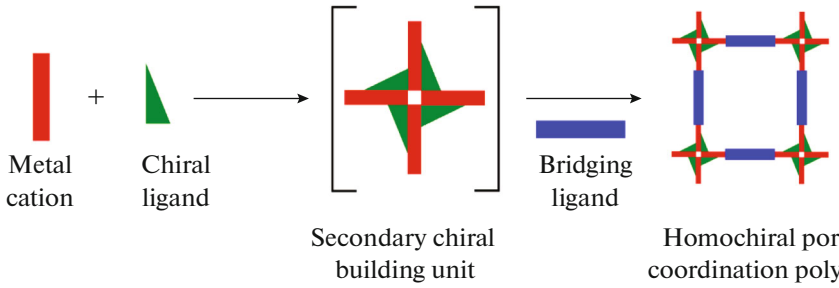

Fig. 6. Scheme of the synthesis of the homochiral porous coordination polymers.

organic frameworks. In fact, if a building unit (motif) will be made chiral, then the structure of the obtained porous framework would contain identical in structure chiral centers. Moreover, the variation of the length or functional substituents of the bridging ligand would allow one to control the size of the channels and the internal environment of the pores.

We pioneered to propose and then experimentally accomplished the rational synthesis of porous homochiral coordination frameworks with the varied structural parameters (Fig. 6) [22], which, in essence, is the development of the Robson and Férey module (block) approach and assumes the use of two organic ligands with different "tasks" in the synthesis. The chiral ligand serves for the introduction of optical centers into the structure due to the formation of coordination complexes with metal cations. These complexes should be of low dimensionality (island 0D, chain 1D, layer 2D), which allows them to be considered as secondary building units (motifs). The connection of these motifs through the bridging ligands in three, two, or one direction would make it possible to organize them into three-dimensional framework structures. Thus, the bridging ligands in the proposed scheme perform an important structure-forming function, since they impart porosity and structural rigidity to the framework and allow one to vary geometric parameters of the cavities due to the changed length of these ligands. A substantial advantage of the proposed approach is the possibility to obtain open porous structures even when using small chiral ligands widely abundant in nature (α-amino acids and others). The aforementioned example of porous camphorates $[M_2(Camph)_2(L)]$ (M = Zn^{2+}, Cu^{2+}; L = Dabco, Bipy, Bpe) is an excellent demonstration of possibilities of our scheme.

Porous homochiral coordination polymers $[Zn_2(DMF)(Xdc)(L)] \cdot x$DMF are formed in the Zn^{2+}–H_2Xdc–H_2L–DMF system (H_2L is *S*-lactic or *R*-mandelic acid) [22, 23]. Chain fragments consisting of zinc(II) cations and the chiral acid residue can be distinguished in the structures of the obtained compounds. These chains act as secondary building units, whose connection through the linear dicarboxylate bridges in two directions forms isotypical homochiral frameworks (Fig. 7). The frameworks contain channels parallel to the chain motifs with a cross section of 4 × 6 Å for $[Zn_2(DMF)(Bdc)(S\text{-Lac})]$ (H_2Lac is lactic acid), 5 × 10 Å for $[Zn_2(DMF)(Ndc)(R\text{-Man})]$ (H_2Man is mandelic acid), and 5 × 14 Å for $[Zn_2(DMF)(R\text{-Man})(Ndc)]$, which is consistent with

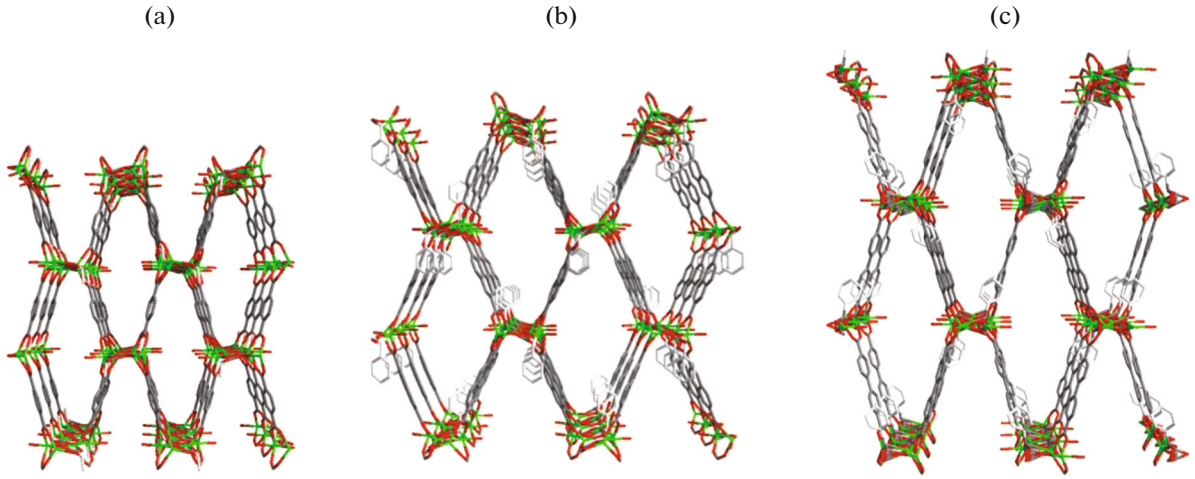

Fig. 7. Structures of the coordination porous homochiral frameworks (a) [Zn_2(DMF)(Bdc)(*S*-Lac)], (b) [Zn_2(DMF)(Ndc)(*R*-Man)], and (c) [Zn_2(DMF)(Bpdc)(*R*-Man)]. The view along the *x* axis (along the chiral chain motifs) is shown.

an increase in the length of the bridging ligand from Bdc^{2-} to Ndc^{2-} and further to $Bpdc^{2-}$ (H_2Bpdc is 4,4'-biphenyldicarboxylic acid). The channels are linked through cross windows with the diameter about 5 Å. The CH_3 and Ph groups of the chiral ligands are directed inside the channels and form an asymmetric environment of the internal surface. In addition, these channels are partially occupied by coordinated DMF molecules.

The reactions of cobalt(II), nickel(II), and copper(II) acetates and/or basic carbonates with *S*-aspartic (H_2Asp) and *S*-malic (H_2Mal) acids in the presence of bridging N-donor ligands (Bipy, Bpe) afforded a series of porous metal-organic coordination polymers of several types (Table 2). The first type is formed by cobalt aspartates and malates [Co_2(*S*-Asp)$_2$(L)] and [Co_2(*S*-Mal)$_2$(L)] (L = Bipy, Bpe), the structure of the metal-organic framework of which is similar to that of nickel and copper aspartates obtained in the Rosseinsky research group [27–29]. The aspartate and malate anions bind the cobalt(II) cations into layers of square topology. These homochiral layers contain chiral centers of only one configuration (Fig. 8). The layers can be considered as secondary building units. The linear bridging ligands (Bipy and Bpe) join the layers into frameworks with the open structure (Fig. 9). Each cobalt cation in this structure is a five-bound node with the shape of a distorted square pyramid. The general topology of the frameworks is described by the point symbol $4^4 6^6$ and has the designation **sqp**. The cross sections of the formed channels are determined by the length of the bridging ligands: 4 × 4 Å for L = Bipy and 4 × 7 Å for L = Bpe.

The structure of nickel(II) malate [Ni_2(*S*-Mal)$_2$(Bipy)] is similar to those of the cobalt(II) compounds described above. The framework [Ni_2(*S*-Mal)$_2$(Bpe)] with a different structure is formed when using the longer Bpe bridge instead of Bipy. As in the previous case, the Ni^{2+} cations and malate anions form chiral layers of square topology, but their structures differ because of the nonequivalence of the Ni^{2+} cations. One cation is coordinated by one α- and three δ-carboxyl groups, whereas another cation, on the contrary, is coordinated by three α-carboxyl groups and one δ-carboxyl group. From the topological point of view, the structures of the networks in [Ni_2(*S*-Mal)$_2$(Bipy)] and in [Ni_2(*S*-Mal)$_2$(Bpe)] are equivalent, but the differences in their structures result in another mode of layer linking into a framework through the linear N-donor ligands. The Bipy ligands are parallel in the framework [Ni_2(*S*-Mal)$_2$(Bipy)], whereas in the structure [Ni_2(*S*-Mal)$_2$(Bpe)] the Bpe ligands are arranged at an angle of 44° to each other

Table 2. Homochiral coordination polymers based on the aspartates and malates

Framework	Framework type	Literature
[Co_2(*S*-Asp)$_2$(Bipy)]	I	[24]
[Co_2(*S*-Asp)$_2$(Bpe)]	I	[24]
[Co_2(*S*-Mal)$_2$(Bipy)]	I	[25]
[Co_2(*S*-Mal)$_2$(Bpe)]	I	[25]
[Ni_2(*S*-Mal)$_2$(Bipy)]	I	[25]
[Ni_2(*S*-Mal)$_2$(Bpe)]	II	[25]
[Ni(*S*-Mal)(Bipy)]	III	[26]
[Ni(*S*-Mal)(Bpe)]	III	[26]
[Cu(*S*-Mal)(Bipy)]	IV	[26]
[Cu(*S*-Mal)(Bpe)]	IV	[26]

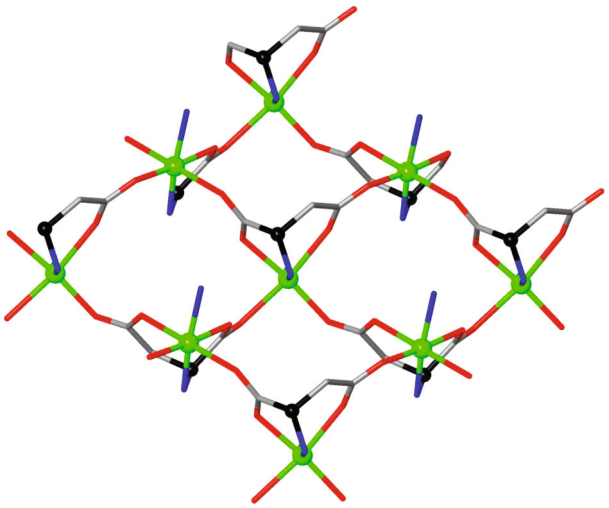

Fig. 8. Fragment of the cobalt aspartate layer {Co(Asp)} in $[Co_2(S\text{-Asp})_2(Bipy)]$ and $[Co_2(S\text{-Asp})_2(Bpe)]$. The cobalt atoms are shown by balls of a larger diameter, and the asymmetric carbon atoms are shown by balls of a smaller diameter.

(Fig. 10). Owing to different modes of bridging ligand packing, the sizes of free passageways in $[Ni_2(S\text{-Mal})_2(Bpe)]$ are 3 × 4 Å, which is somewhat smaller than those for structure $[Ni_2(S\text{-Mal})_2(Bipy)]$, in spite of the shorter length of the bridge (4 × 4 Å).

Nickel(II) malates with different compositions and structures were obtained under similar experimental conditions: [Ni(*S*-Mal)(Bipy)] and [Ni(*S*-Mal)(Bpe)]. Each malate anion is a tridentate chelate-bridging ligand that links two nickel cations (one nickel cation is linked monodentately, and another is bound through the tridentate mode). The Ni^{2+} cations and *S*-Mal^{2-} anions form chiral chains {Ni(*S*-Mal)} along the crystallographic *x* axis. Malic acid residues in these chains are arranged according to the "head-to-tail" principle. The chiral chains are linked by the linear bridging ligands in two directions to form a homochiral framework with the open structure (Fig. 11). In this structure, each Ni atom can be simplified to a four-bound node. The latter are connected through two malate and two N-donor bridges into a four-bound lattice with the diamond topology **dia**. Two types of intersecting channels can be distinguished in the [Ni(*S*-Mal)(Bipy)] and [Ni(*S*-Mal)(Bpe)] frameworks: the channels directed along the *x* axis and along the volume diagonals with a cross section of 5 × 4 and 4 × 4 Å for the former and of 7 × 7 and 5 × 5 Å for the latter.

The reaction of binuclear copper(II) acetate $[Cu_2(OAc)_2(H_2O)_2]$ with malic acid in the presence of an N-donor ligand affords porous malates [Cu(*S*-Mal)(L)] (L = Bipy, Bpe) with similar compositions but different structures of the metal-organic framework. The copper(II) cations and malate anions form chiral layers {Cu(*S*-Mal)} with the honeycomb structure and a topology of (6,3)-networks and acting as secondary chiral building unit. The linear N-donor ligands Bipy or Bpe bind the chiral layers {Cu(*S*-Mal)} into isoreticular homochiral framework structures [Cu(*S*-Mal)(Bipy)] and [Cu(*S*-Mal)(Bpe)] (Fig. 12). In the coordination frameworks, the nodes corresponding to the copper cations are five-bound. Thus, the frameworks of copper(II) malates [Cu(*S*-Mal)(L)]

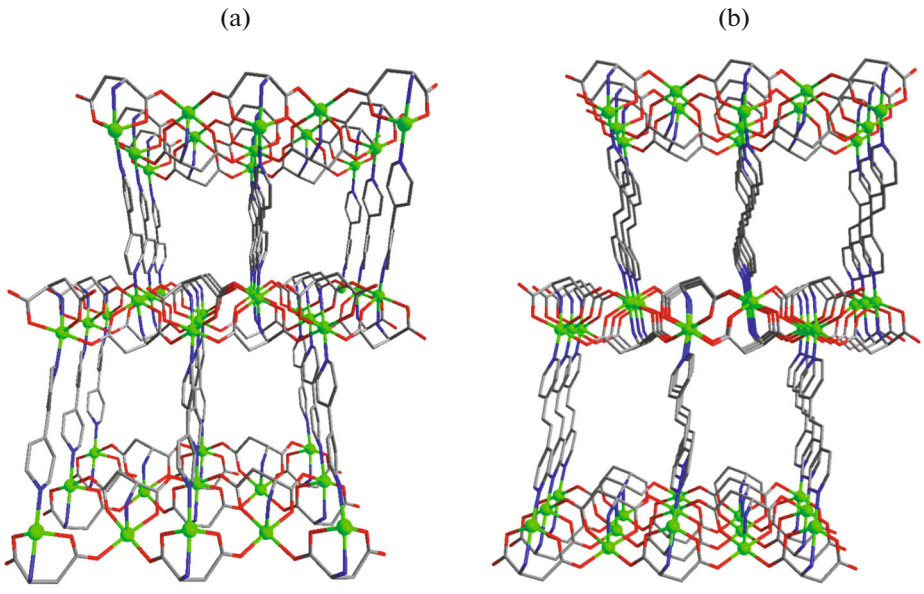

Fig. 9. Structure of the metal-organic frameworks (a) $[Co_2(S\text{-Asp})_2(Bipy)]$ and (b) $[Co_2(S\text{-Asp})_2(Bpe)]$. The view with prospect along the {Co(Asp)} layers is shown. The cobalt atoms are shown by balls.

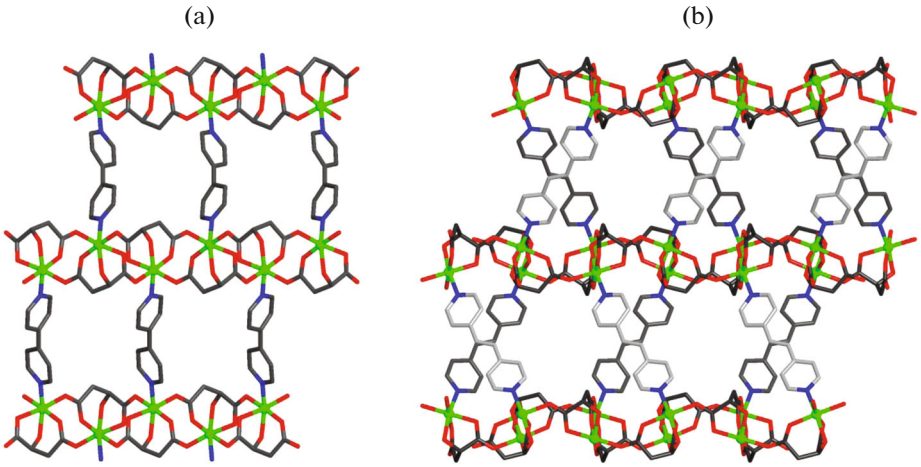

Fig. 10. Comparison of the structures of the metal-organic frameworks (a) $[Ni_2(S\text{-Mal})_2(Bipy)]$ and (b) $[Ni_2(S\text{-Mal})_2(Bpe)]$. The nickel atoms are shown by balls. The view of the channels along the *y* axis is given. Some intersecting (in the projection) Bpe ligands are shown by a lighter tint for clarity.

are classified as two-nodal (3,5)-bound lattices with the **hms** topology and point symbol $(6^3)(6^9.8)$. A similar framework was described for copper tartrates [Cu(Tart)(L)] (H_2Tart is tartaric acid; L = Bipy, Bpe), but its topology was assigned incorrectly [30]. Cavities with a characteristic size of 5 × 5 × 6 and 5 × 5 × 9 Å can be distinguished in the interframe space of copper(II) malates [Cu(*S*-Mal)(Bipy)] and [Cu(*S*-Mal)(Bpe)], respectively. As can be seen from these data, the elongation of the bridging ligand L regularly increases the size of the cavities. The cavities are separated from each other by small passageways (diameter not more than 3 Å) and filled with water molecules.

REMOVAL AND EXCHANGE OF GUESTS AND GAS SORPTION PROPERTIES

The ancestor of the series, $[Zn_2(Bdc)_2(Dabco)]$, is most studied [16] in the series of the $[Zn_2(Xdc)_2(L)]$ frameworks. Since this compound is obtained by the solvothermal reaction in a DMF solution, the channels of the metal-organic framework are filled with solvent molecules. The composition of the obtained compound is $[Zn_2(Bdc)_2(Dabco)] \cdot 4DMF \cdot 1/2H_2O$. Guest (solvent) molecules can be removed on heating in a dynamic vacuum. This gives a permanently stable porous framework with free channels, which can again be filled with molecules of guests of different types. The inclusion, removal, and substitution of the latter are reversible without metal-organic framework decomposition. In this process, the metal-organic framework $[Zn_2(Bdc)_2(Dabco)]$ demonstrates some flexibility, in spite of the fact that the framework is built of fairly rigid fragments. The empty framework contains regular square channels. The framework walls are deformed upon the inclusion of DMF molecules (Fig. 13), and the cell volume decreases by nearly 5% relative to the empty framework. Inclusion compound $[Zn_2(Bdc)_2(Dabco)] \cdot 2C_6H_6$ is formed on the storage of $[Zn_2(Bdc)_2(Dabco)]$ in liquid benzene. The inclusion of benzene molecules also leads to the deformation of the initial framework but of another type. The terephthalate layer undergoes rhombic distortion (Fig. 13). After the guest molecules were removed, the metal-organic framework recovered the initial symmetric shape.

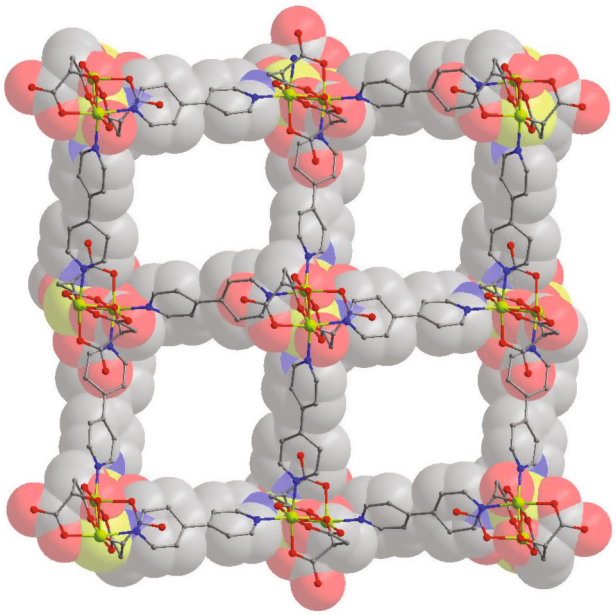

Fig. 11. Coordination homochiral framework [Ni(*S*-Mal)(Bipy)]. The view along the chiral {Ni(*S*-Mal)} chains is given. The ball-and-stick model is shown against the background of the van der Waals diameters of the atoms.

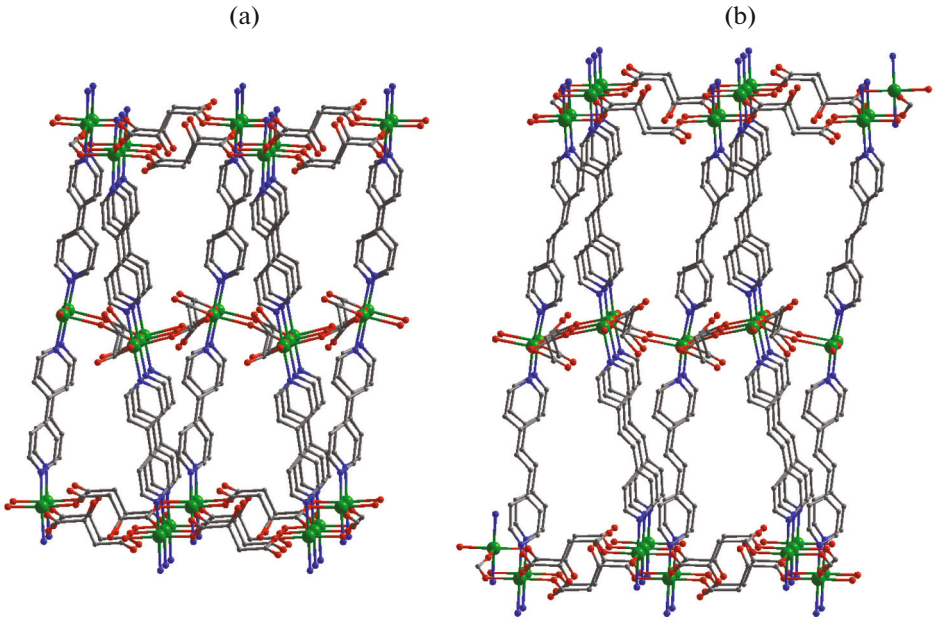

Fig. 12. Structures of the coordination homochiral frameworks (a) [Cu(*S*-Mal)(Bipy)] and (b) [Cu(*S*-Mal)(Bpe)]. The view along the {Cu(*S*-Mal)} layers is given.

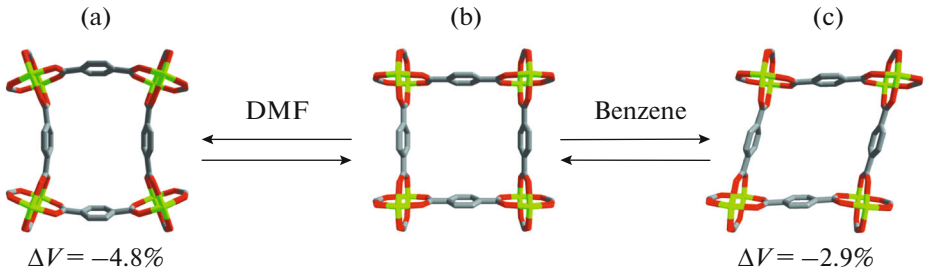

Fig. 13. Fragments of the crystal structures of the $\{Zn_2(Bdc)_2\}$ layer for (a) $[Zn_2(Bdc)_2(Dabco)] \cdot 4DMF \cdot 1/2H_2O$, (b) $[Zn_2(Bdc)_2(Dabco)]$, and (c) $[Zn_2(Bdc)_2(Dabco)] \cdot 2C_6H_6$ showing reversible distortions in the structure upon the introduction of various guest molecules into the cavities of $[Zn_2(Bdc)_2(Dabco)]$. Numbers show the changes in the specific unit cell volumes relative to the porous framework $[Zn_2(Bdc)_2(Dabco)]$.

The permanent porosity of the $[Zn_2(Bdc)_2(Dabco)]$ framework is also confirmed by the data obtained from the nitrogen and hydrogen adsorption isotherms at 77 K and the pressure up to 1 bar [16]. The measurements show reversible sorption–desorption. The nitrogen adsorption isotherm belongs to type I according to the IUPAC classification, which is characteristic of microporous sorbents. The specific surface area calculated using the Brunauer–Emmett–Teller (BET) model is 1450 m^2/g. In addition, methane adsorption in $[Zn_2(Bdc)_2(Dabco)]$ was studied in detail in the pressure range up to 35 bar at temperatures of 198, 223, 273, and 296 K (Fig. 14) [31]. The isotherm curves are reversible and belong to type I. The adsorption isotherm at 198 K achieves saturation at the pressure higher than 17 bar. The maximum amount of sorbed methane corresponds to 6.8 CH_4 molecules per formula unit of the $[Zn_2(Bdc)_2(Dabco)]$ framework.

The adsorption sites of methane in $[Zn_2(Bdc)_2(Dabco)]$ were studied in detail by X-ray crystallography [31]. The framework cavities contain three types of localization sites for CH_4 molecules. The sites of the first type are localized on the mirror planes near the structural units $\{Zn_2(COO)_4\}$ and interact with the O atoms of the binuclear fragments $\{Zn_2(COO)_4\}$ (C···O 3.74 Å) and with the benzene ring of the Bdc^{2-} ligand (C···C 3.33 Å) due to van der Waals contacts. Methane molecules of the second type lie on the mirror planes between Dabco and Bdc^{2-} (C···C 3.99 Å). Methane molecules of the third type are arranged at the center of the cavity, where they form weak secondary contacts with other CH_4 molecules

(C···C 4.02 and 3.91 Å). Taking into account the number of sites per formula unit $[Zn_2(Bdc)_2(Dabco)]$ and their occupancies, the total number of methane molecule is equal to 6.69 and corresponds to the value obtained from the data on methane adsorption at 198 K.

The sorption properties of other porous frameworks of the family $[Zn_2(Xdc)_2(L)_2]$ (Xdc = Me_4Bdc, 1/2Me_4Bdc + 1/2Bdc, Ph-Bdc, F_4Bdc; L = Dabco or Bipy) with respect to nitrogen and hydrogen at T = 77 K and $P \leqslant 1$ bar were also studied [17]. The sorption characteristics of the studied porous coordination polymers are summarized in Table 3. In all cases, the nitrogen adsorption isotherms showed saturation in the range of low pressures (up to 0.1 bar), which is characteristic of microporous compounds. The total pore volume of coordination polymers varies from 0.50 to 0.62 mL/g, which is noticeably larger than that for microporous zeolites (0.05–0.25 mL/g). The calculated values of specific surface area (according to the BET model) range from 920 to 1450 m^2/g. Evidently, the introduction of substituents into the $[Zn_2(Bdc)_2(Dabco)]$ framework results in somewhat decrease in the cavity sizes and an increase in the gravimetric density, which decreases, as a whole, the specific sorption characteristics. Interestingly, the calculation of the number of N_2 molecules per formula unit $[Zn_2(Xdc)_2(L)]$ shows that this decrease in the specific surface and cavity sizes does not significantly affect the amount of adsorbed N_2. Moreover, $[Zn_2(Bdc)_2(Dabco)]$, being the most porous framework in the presented family, shows a slightly smaller amount of sorbed N_2 compared to other denser frameworks.

The data presented demonstrate that the functionalization of the bridging ligands can noticeably enhance the interaction between the gas and adsorbent. The curves of hydrogen adsorption by $[Zn_2(Xdc)_2(L)_2]$ at 77 K are pronouncedly unsaturated, which is typical of any porous material. In the approximation of the Langmuir model (monolayer coating of the surface), the obtained isotherms were used to calculate the constants for the equation of the adsorption isotherm: $S = S_{max}K_aP/(K_aP + 1)$, where S is the amount adsorbed at the current pressure (P), S_{max} is the theoretical saturated amount adsorbed at an infinite pressure, and K_a is the Langmuir adsorption constant (in the range of low pressures, in essence, corresponding to the Henry constant). As can be seen from the data presented, the functionalization of the $[Zn_2(Bdc)_2(Dabco)]$ framework enhances indeed the affinity to H_2. The most noticeable effect is made by methyl groups, the introduction of which appreciably increases the adsorption constants of the $[Zn_2(MeBdc)_2(Dabco)]$ and $[Zn_2(Me_4Bdc)_2(Bipy)]$ frameworks in the range of low H_2 pressures, where the amount of adsorbed hydrogen molecules is determined by the presence of stronger sorption sites. As the pressure increases, hydrogen adsorption depends on the specific surface, since at low temperatures

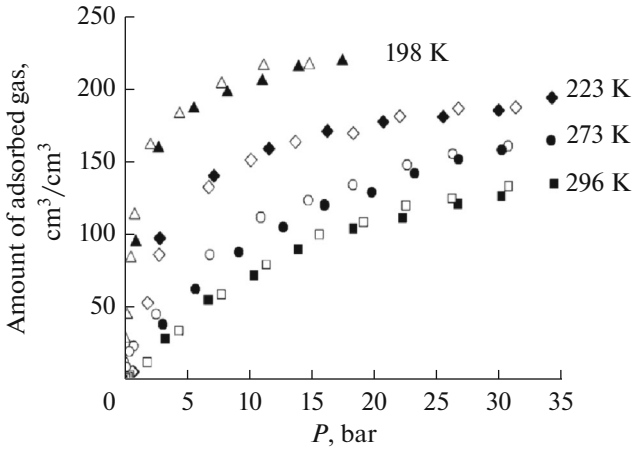

Fig. 14. Isotherms of methane adsorption by the $Zn_2(Bdc)_2(Dabco)]$ framework at different temperatures.

Table 3. Sorption characteristics of the microporous coordination polymers

Compound	S_a (L)[a] m^2/g	S_a (BET)[b] m^2/g	V_p[c] mL/g	V_p[d] mL/mL	Number of N_2 molecules per formula unit[e]	Number of H_2 molecules per formula unit[f]	K_a[g]
$[Zn_2(Bdc)_2(Dabco)]$	2090	1450	0.75	0.62	12.3	5.7	0.73
$[Zn_2(Bdc)(Me_4Bdc)(Dabco)]$	1670	1100	0.59	0.54	10.7	6.5	3.3
$[Zn_2(Me_4Bdc)_2(Dabco)]$	1400	920	0.50	0.50	9.9	6.2	8.9
$[Zn_2(Ph\text{-}Bdc)_2(Dabco)]$	1450	1000	0.52	0.50	10.1	5.7	3.3
$[Zn_2(F_4Bdc)_2(Dabco)]$	1610	1070	0.57	0.59	11.9	6.3	1.3
$[Zn_2(Me_4Bdc)_2(Bipy)]$	1740	1120	0.62	0.45	13.0	6.1	4.2

[a] Specific surface area according to the Langmuir model calculated from the isotherm of N_2 adsorption; [b] specific surface area according to the BET model calculated from the isotherm of N_2 adsorption; [c] gravimetric pore volume; [d] volumetric pore volume; [e] at saturation (0.95 bar, 77 K); [f] at 1 atm, 77 K; [g] hydrogen adsorption constant calculated using the Langmuir model.

(77 K) H_2 molecules form a monolayer regardless of the strength of H_2 binding with the porous sorbent surface already in the range up to 10 bar.

The framework structure is retained upon an attempt to remove guest molecules only for $[Zn_2(Camph)_2(Dabco)]$ among all porous zinc camphorates $[Zn_2(Camph)_2(L)] \cdot xG$ (G = DMF, H_2O; L = Dabco, Bipy, Bpe), whereas $[Zn_2(Camph)_2(Bipy)]$ and $[Zn_2(Camph)_2(Bpe)]$ undergo amorphization [19]. The permanent porosity of the $[Zn_2(Camph)_2(Dabco)]$ framework was confirmed by measuring the N_2 adsorption isotherm, showing a specific surface area of 553 m^2/g (in terms of the Langmuir model). The pure porous $[Zn_2(Camph)_2(Bipy)]$ framework can be obtained by the activation of an intermediate compound, which was prepared by immersion of the initial coordination polymer in CH_2Cl_2, in vacuo at room temperature. According to the nitrogen adsorption data, $[Zn_2(Camph)_2(Bipy)]$ demonstrates the reversible isotherm of type I typical of microporous materials. The calculated specific surface area (according to the Langmuir model) was 1014 m^2/g, which is more expectable than the value in the case of $[Zn_2(Camph)_2(Dabco)]$. Thus, the stability of the frameworks of porous zinc camphorates $[Zn_2(Camph)_2(L)]$ is determined by the length and nature of bridging ligand L. In the case of short L (Dabco), the framework structure is permanently porous and resistant to guest removal at high temperatures. In the case of longer L (Bipy), the framework is resistant to the exchange of guests and activation under mild conditions. The framework loses crystallinity at elevated temperatures but can reversibly be regenerated under the action of a solvent. In the case of the longest bridge, the $[Zn_2(Camph)_2(Bpe)]$ framework is unstable even under mild conditions of guest exchange, and its degradation is irreversible.

In the freshly synthesized compounds $[Zn_2(DMF)(Bdc)(S\text{-Lac})] \cdot DMF$, $[Zn_2(DMF)(Ndc)(R\text{-Man})] \cdot 3DMF$, and $[Zn_2(DMF)(Ndc)(R\text{-Man})] \cdot 2DMF$, the channels are occupied by solvent molecules (DMF) [22, 23]. The compounds lose solvent molecules in a range of 100–200°C. It seems impossible to separate the processes of removing of guest and similar coordinated molecules into distinct steps. The storage of crystals $[Zn_2(DMF)(Bdc)(S\text{-Lac})] \cdot DMF$ in a dynamic vacuum at room temperature and with a gradual temperature increase results in the broadening of and a decrease in the reflection intensity in the X-ray powder pattern. The adsorption of H_2 was measured for the partially activated framework $[Zn_2(DMF)_x(Bdc)(S\text{-Lac})] \cdot yDMF$ ($x + y \approx 1$) at $T = 77$ K and the specific surface area was calculated to be 190 m^2/g. Such a low value indicates a low stability of the activated framework. Deeper activation leads to the complete degradation of the framework.

CATALYSIS AND SEPARATION OF ENANTIOMERS

The use of porous homochiral coordination polymers in the processes of fine purification or catalysis does not require the presence of highly stable permanently porous frameworks, since all these processes are often carried out at room temperature and in the presence of a solvent. The catalytic properties of the homochiral porous coordination polymers toward the oxidation of nonsymmetric sulfides were studied for compounds $[Zn_2(DMF)(Xdc)(L)] \cdot xDMF$ (Xdc = Bdc, Ndc, Bpdc; L = *S*-Lac, *R*-Man) [22, 23, 32, 33].

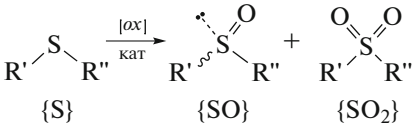

Important products of this reaction are sulfoxides with mirror asymmetry, since they are precursors for a series of important chiral drugs (Omeprazole, Sulforaphane, Armodafinil). Nonsymmetric sulfides were taken as substrates: methyl phenyl sulfide (PhSMe), *para*-bromophenyl methyl sulfide (p-BrC_6H_4SMe), *para*-nitrophenyl methyl sulfide (p-$NO_2C_6H_4SMe$), benzyl phenyl sulfide ($PhSCH_2Ph$), and methyl 2-naphthyl sulfide (2-NaphSMe). Hydrogen peroxide and its complex with urea were used as oxidants. The reactions were carried out in a solution of acetonitrile or dichloromethane. The key parameters of the studied processes are the total conversion characterizing the depth of initial sulfide oxidation and the selectivity to sulfoxide characterizing the fraction of the target sulfoxide in a mixture of oxidation products. The additional experiments performed show that all catalytic reactions proceed in the heterogeneous regime, indicating a high stability of the metal-organic frameworks under the reaction conditions. The results of the catalytic oxidation of the sulfides are given in Table 4.

The presented data show that the studied coordination polymers exhibit high catalytic activity in the oxidative synthesis of the sulfoxides. A deep conversion (>90%) at the 100% selectivity of oxidation can be achieved under the most optimum conditions; i.e., sulfoxide is the single reaction product. These values are comparable with those characteristic of the best homogeneous catalysts. The studied compounds can experience up to 15 catalytic cycles. A significant relationship between the size of the substrate and its conversion is observed for the porous framework $[Zn_2(DMF)(Bdc)(S\text{-Lac})]$ having small cavities of ~5 Å. A higher (more than 90%) conversion can be achieved in oxidation in many experiments for sulfoxides with a smaller size (PhSMe or p-BrC_6H_4SMe). At the same time, the maximum conversion is only

Table 4. Data on the catalytic oxidation of sulfides in the presence of the chiral coordination polymers

Substrate	Catalyst[a]	Oxidant	S : {cat} : {ox}[b]	Solvent	Total conversion, %[c]	Selectivity, %[c]
PhSMe	ZBL*	H_2O_2 (30%)	1.5 : 1 : 4.5	CH_3CN	92	100
PhSMe	ZBL*	UHP	1 : 1 : 2	CH_2Cl_2	64	92
PhSMe	ZBL*	H_2O_2 (90%)	1.5 : 1 : 4.5	CH_3CN/CH_2Cl_2 (1 : 10)	100	87
PhSMe	ZBL	UHP	1.5 : 1 : 4.5	CH_3CN	92	100
PhSMe	ZBL	UHP	5 : 1 : 7.5	CH_3CN	94	98
p-BrC_6H_4SMe	ZBL*	H_2O_2 (90%)	25 : 1 : 75	CH_3CN/CH_2Cl_2 (1 : 10)	58	100
p-BrC_6H_4SMe	ZBL*	H_2O_2 (90%)	1.5 : 1 : 4.5	CH_3CN/CH_2Cl_2 (1 : 10)	85	100
p-BrC_6H_4SMe	ZBL*	UHP	1 : 1 : 2	CH_2Cl_2	58	83
p-BrC_6H_4SMe	ZBL*	H_2O_2 (30%)	1.5 : 1 : 4.5	CH_3CN	8	100
p-$NO_2C_6H_4SMe$	ZBL*	UHP	1 : 1 : 2	CH_2Cl_2	7	90
$PhSCH_2Ph$	ZBL*	UHP	1 : 1 : 2	CH_2Cl_2	3	[d]
$PhSCH_2Ph$	ZNM	UHP	12.5 : 2 : 25	CH_3CN	70	99
2-NaphSMe	ZNM	UHP	12.5 : 2 : 25	CH_3CN	78	99
$PhSCH_2Ph$	ZBpM	UHP	12.5 : 2 : 25	CH_3CN	78	98.5
2-NaphSMe	ZBpM	UHP	12.5 : 2 : 25	CH_3CN	57	98

ZBL* = $[Zn_2(DMF)(Bdc)(S\text{-Lac})] \cdot 0.4DMF$; ZNM = $[Zn_2(DMF)(Ndc)(R\text{-Man})] \cdot 3DMF$; ZBpM = $[Zn_2(DMF)(Bpdc)(R\text{-Man})] \cdot 2DMF$; [a] ZBL = $[Zn_2(DMF)(Bdc)(S\text{-Lac})] \cdot DMF$; [b] molar ratio substrate/catalyst (formula unit)/oxidant; [c] conversion = $(\{SO\} + \{SO_2\})/(\{S\} + \{SO\} + \{SO_2\}) \times 100\%$; selectivity = $\{SO\}/(\{SO\} + \{SO_2\}) \times 100\%$, where {S}, {SO}, and $\{SO_2\}$ designate the amounts of sulfide, sulfoxide, and sulfone, respectively; [d] was not determined because of a low yield.

7 and 3% for sulfides with a large size of substituents (p-$NO_2C_6H_4SMe$ or $PhSCH_2Ph$, respectively). Such a sharp dependence of the efficiency of heterogeneous catalysis on the substrate size can indicate that catalytic activation occurs mainly inside the porous framework rather than on the crystal surface. The inclusion of the substrate into the chiral cavities of $[Zn_2(DMF)(Bdc)(S\text{-Lac})]$ is the necessary condition for catalytic oxidation to occur. The frameworks with larger cavities, $[Zn_2(DMF)(Ndc)(R\text{-Man})]$ and $[Zn_2(DMF)(Bpdc)(R\text{-Man})]$, show a significant efficiency in the oxidation of large sulfides $PhSCH_2Ph$ and 2-NaphSMe (conversion from 57 to 78%). Thus, the compounds obtained by us exhibit the high activity in the heterogeneous catalytic oxidation of sulfides due to the stable porous crystal structure with the regular size of the channels. The catalytic process is characterized by a high selectivity to the substrate size and a high yield of the target product (sulfoxide). Note that the homochiral porous coordination polymer $[Zn_2(DMF)(Bdc)(S\text{-Lac})] \cdot DMF$ and its isoreticular analogs are the first example of the heterogeneous Zn-containing catalysts for sulfide oxidation combining a high conversion, selectivity to the substrate size, and almost no by-products. A substantial drawback of the studied reactions is the absence of enantiomeric excess in the sulfoxide products; i.e., they are formed as racemic mixtures, in spite of the fact that catalysis occurs mainly inside the chiral cavities.

The stereoselective sorption properties toward racemic mixtures of various substrates (sulfoxides and alcohols) were studied for the homochiral porous coordination polymers $[Zn_2(DMF)(Bdc)(S\text{-Lac})] \cdot DMF$, $[Zn_2(DMF)(Ndc)(R\text{-Man})] \cdot 3DMF$, and $[Zn_2(Dmf)(Ndc)(R\text{-Man})] \cdot 2DMF$.

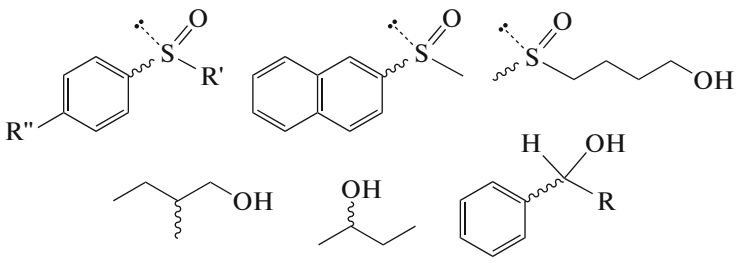

The experimental data are summarized in Table 5. Note that the sorption properties of $[Zn_2(DMF)(Bdc)_2(S\text{-Lac})]$ after its multiple use and regeneration are identical to those for the initial sample, indicating a high stability of the coordination frameworks under the experimental sorption conditions. As can be seen from the comparison of the presented data, the studied porous structures exhibit selectivity of sorption depending on the substrate sizes. For example, the $[Zn_2(DMF)(Bdc)(S\text{-Lac})]$ framework rather well sorbs sulfoxides with small substituents (PhSOMe, p-MeC_6H_4SOMe, PhSO-*iso*-Pr, $MeSO(CH_2)_4OH$), whereas the introduction of larger substituents makes the sorption insignificant or impossible at all (p-NO_2-C_6H_4SOMe, 2-NaphSOMe). An increase in the cavity sizes in the homochiral frameworks results in a regular increase in the sizes of the substrates that can enter these pores. The $[Zn_2(DMF)(Bdc)(S\text{-Lac})]$ framework with the smallest pores badly sorbs fairly large substrate 2-NaphSOMe, whereas more porous frameworks $[Zn_2(DMF)(Ndc)(R\text{-Man})]$ and $[Zn_2(DMF)(Bpdc)(R\text{-Man})]$ show good adsorption of this guest. The structure of the chiral center indirectly affects the geometry of the guest having the preferable affinity to the homochiral porous framework. It is well seen that the *S*-configuration of lactate in $[Zn_2(Bdc)(S\text{-Lac})(DMF)]$ results in the preferable sorption of *S*-forms of sulfoxides, whereas the *R*-configuration of mandelate in $[Zn_2(Ndc)(R\text{-Man})(DMF)]$ and $[Zn_2(Bpdc)(R\text{-Man})(DMF)]$ results in the preferential sorption of *R*-sulfoxides. Another important conclusion is the fact that the best correspondence of the sizes of the porous sorbent and substrate is necessary to achieve the highest efficiency (*ee*) in stereoselective sorption. This general regularity has been observed long ago for various systems and is explained by the necessity of a tighter interaction in the substrate–sorbent pair, which is attained for the close correspondence of the sizes.

The methods developed by us for the synthesis of homochiral coordination polymers make it possible to obtain them in one step in the crystalline state from available reagents in a yield scaled to hundreds of grams. This allowed us to synthesize a sufficient amount of $[Zn_2(DMF)(Bdc)(S\text{-Lac})] \cdot DMF$ and to prepare a chromatographic column for the preparative separation of racemic mixtures of various sulfoxides [32]. Racemic mixtures of nonsymmetric sulfoxides PhSOMe, p-MeC_6H_4SOMe, p-BrC_6H_4SOMe, and PhSO-*iso*-Pr were used for separation. The efficiency of separation directly correlates with the data on *ee* for static sorption experiments. The best result was obtained for PhSOMe, whose individual isomers can completely be separated by chromatography. A good but not complete separation of the peaks is observed in the case of PhSO-*iso*-Pr. The chromatographic results are consistent with the sorption data in the sense that the *S*-isomer necessarily has a higher retention time than that of the *R*-isomer. This indicates a higher affinity of *S*-sulfoxide to the $[Zn_2(DMF)(Bdc)(S\text{-Lac})] \cdot DMF$ framework.

The quantitative simulation of the chiral host–chiral guest interaction was performed for the $[Zn_2(DMF)(Bdc)(S\text{-Lac})]$–PhSOMe system using quantum-chemical methods based on the first principles (ab initio). The data of theoretical calculations agree with the results of sorption experiments: host–guest interactions are favorable only for *S*-PhSOMe ($E_{ads} = -1.568$ kcal/mol), whereas these interactions are repulsive in character for *R*-PhSOMe [23]. An analysis of interatomic distances in the optimized structures shows that the formation of a C–H···O hydrogen bond between the methyl group of the DMF ligand and the oxygen atom of the sulfoxide molecule is the determining factor in the stability of the corresponding host–guest complex.

The nature of chiral guest–chiral framework interactions was also studied by single-crystal X-ray crystallography [34]. The samples for X-ray diffraction were obtained by the storage of single crystals of $[Zn_2(DMF)(Bdc)(S\text{-Lac})] \cdot DMF$ in *S*-PhMeCHOH or *R*-PhMeCHOH for 48 h. According to the X-ray diffraction data, the replacement of the guest DMF molecule in the porous framework by PhMeCHOH does not provide any substantial changes in the structure of the coordination framework. The guest molecules *S*-PhMeCHOH or *R*-PhMeCHOH occupy close positions at the center of the cavity with a similar orientation of the methyl and phenyl groups. A significant distinction appears only as an orientation of the hydroxyl group of alcohol and its interaction with different fragments of the framework (Fig. 15). In compound $[Zn_2(DMF)(Bdc)(S\text{-Lac})] \cdot R\text{-PhMeCHOH}$, the OH-group forms short contacts with the carboxylic oxygen atoms (O···O 3.26 and 3.35 Å), whereas the hydroxyl group in complex $[Zn_2(DMF)(Bdc)(S\text{-Lac})] \cdot S\text{-PhMeCHOH}$ forms a short contact with the hydrogen atoms of the methyl group of the coordinated DMF ligand (O···C 3.33 Å). In spite of relatively longer distances in these contacts, they are the shortest and most significant interatomic distances in host–guest complexes and, most likely, cause stereodifferentiation. The independent experimental methods (polarimetry, high-performance liquid chromatography, differential scanning calorimetry) unambiguously prove a higher affinity of the $[Zn_2(DMF)(Bdc)(S\text{-Lac})]$ framework to *S*-PhMeCHOH. This means that the interaction between the chiral guest molecule and coordinated DMF ligand of the framework plays the determining role in the stabilization of the structure $[Zn_2(DMF)(Bdc)(S\text{-Lac})] \cdot S\text{-PhMeCHOH}$.

The X-ray diffraction data and theoretical studies confirm a substantial role of weak interatomic interactions in the stereospecific recognition of chiral mole-

Table 5. Experimental data on stereoselective sorption

Sorbent[a]	Substrate[b]	Solvent	Adsorption, molecules per formula unit[c]	*ee*, %[d]	Preferably sorbed isomer[e]
ZBL · 0.4DMF	PhSOMe	CH_2Cl_2	0.68	20	*S*
ZBL · 0.4DMF	*p*-BrC_6H_4SOMe	CH_2Cl_2	0.18	27	*S*
ZBL · 0.4DMF	*p*-NO_2-C_6H_4SOMe	CH_2Cl_2	~0	[f]	
ZBL · 0.4DMF	$PhSOCH_2Ph$	CH_2Cl_2	~0	[f]	
ZBL · 0.4DMF [g]	*p*-BrC_6H_4SOMe	CH_2Cl_2	0.18	? [h]	
ZBL(act) [i]	*p*-BrC_6H_4SOMe	CH_2Cl_2	0.05	12	*S*
ZBL · DMF	*p*-BrC_6H_4SOMe	CH_2Cl_2	0.3	7	*S*
ZBL · DMF	PhSOMe	CH_2Cl_2	0.30	60	*S*
ZBL · DMF	*p*-MeC_6H_4SOMe	CH_2Cl_2	0.53	38	*S*
ZBL · DMF	*p*-NO_2-C_6H_4SOMe	CH_2Cl_2	~0	[f]	
ZBL · DMF	PhSO-*iso*-Pr	CH_2Cl_2	0.25	54	*S*
ZBL · DMF	2-NaphSOMe	CH_2Cl_2	0.13	[f]	
ZBL · DMF	$MeSO(CH_2)_4OH$	CH_2Cl_2	0.65	20	*R*
ZBL · DMF	MeCH(OH)Et	[j]	1	14	*R*
ZBL · DMF	MeCH(OH)Et	[j]	1	7	*R*
ZBL · DMF	PhMeCHOH	[j]	1	21	*S*
ZBL · DMF	PhPrOH	[j]	0.75	12	*S*
ZNM · 3DMF	PhSOMe	CH_2Cl_2	0.36	19	*R*
ZNM · 3DMF	PhSO-*iso*-Pr	CH_2Cl_2	0.16	15	*R*
ZNM · 3DMF	PhSO-*iso*-Pr	CH_3CN	0.51	62	*R*
ZNM · 3DMF	$PhSOCH_2Ph$	CH_2Cl_2	0.13	0	
ZNM · 3DMF	2-NaphSOMe	CH_3CN	0.72	17	*R*
ZNM · 3DMF	2-NaphSOMe	CH_2Cl_2	0.48	31	*R*
ZBpM · 2DMF	PhSOMe	CH_2Cl_2	0.08	12	*R*
ZBpM · 2DMF	PhSO-*iso*-Pr	CH_3CN	0.13	7	*S*
ZBpM · 2DMF	PhSO-*iso*-Pr	CH_2Cl_2	0.02	[f]	
ZBpM · 2DMF	$PhSOCH_2Ph$	CH_2Cl_2	0.05	0	
ZBpM · 2DMF	2-NaphSOMe	CH_3CN	0.44	27	*R*

[a] The following designations were used: ZBL = [Zn_2(DMF)(Bdc)(*S*-Lac)]; ZNM = [Zn_2(DMF)(Ndc)(*R*-Man)]; ZBpM = [Zn_2(DMF)(Bpdc)(*R*-Man)]; [b] structures of the substrates are presented in the page 570; [c] shows the number of sorbed substrate molecules per formula unit of the framework equivalent to 2 Zn atoms; [d] enantiomeric excess was calculated using the formula *ee* = ([S] – [R])/([S] + [R]) × 100%, where [R] and [S] correspond to the amounts of the *R*- and *S*-forms, respectively, of the substrate sorbed inside the porous framework; [e] shows the form of the substrate preferably sorbed by the porous framework; [f] no adsorption or adsorption is so negligible that cannot be determined; [g] regenerated framework was used; [h] *ee* was not determined; [i] activated [$Zn_2(Bdc)_2$(*S*-Lac)(DMF)*x*] framework, where $x < 1$, was used; [j] pure liquid substrates without a solvent were used.

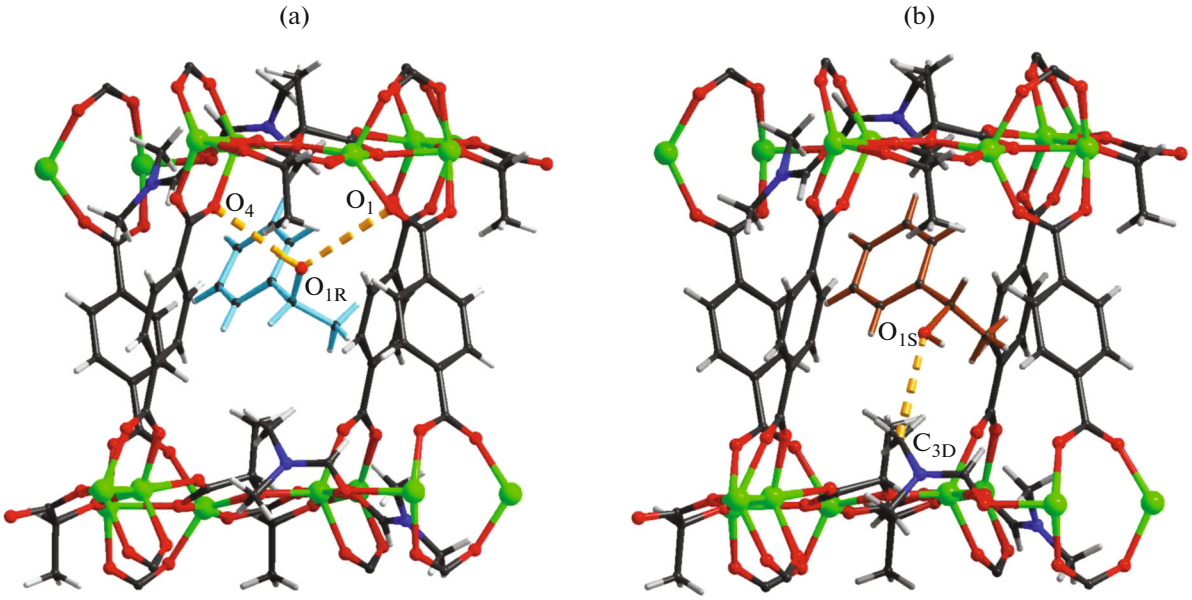

Fig. 15. Structures of the host–guest complexes for (a) $[Zn_2(DMF)(Bdc)(S\text{-Lac})] \cdot R\text{-PhMeCHOH}$ and (b) $[Zn_2(DMF)(Bdc)(S\text{-Lac})] \cdot S\text{-PhMeCHOH}$.

cules, where coordinated DMF molecules play a special role. The formation of weak C–H···O bonds between the guest molecule and the methyl group of the coordinated DMF ligand in the homochiral framework $[Zn_2(DMF)(Bdc)(S\text{-Lac})]$ plays the decisive role in stereoselective processes.

Thus, the carboxylate complexes play an exclusively important role in the development of the chemistry of porous metal-organic coordination polymers, including homochiral ones. Polycarboxylate ligands are easily available or can be synthesized rather simply. The most numerous families of permanently porous electroneutral frameworks with an enhanced robustness to the removal of guest molecules were obtained using the polycarboxylate ligands. Classical coordination chemistry of the carboxylate complexes of transition (and nontransition) metals is well studied, which makes it possible to perform the design–directed synthesis of isoreticular coordination frameworks for the solution of problems of selective sorption, separation, and catalysis.

ACKNOWLEDGMENTS

This work was supported by the Russian Foundation for Basic Research, project no. 14-03-00141.

REFERENCES

1. Hoskins, B.F. and Robson, R., *J. Am. Chem. Soc.*, 1989, vol. 111, p. 5962.
2. Hoskins, B.F. and Robson, R., *J. Am. Chem. Soc.*, 1990, vol. 112, p. 1546.
3. Blake, A.J., Champness, N.R., Hubberstey, P., et al., *Coord. Chem. Rev.*, 1999, vol. 183, p. 117.
4. Khlobystov, A.N., Blake, A.J., Champness, N.R., et al., *Coord. Chem. Rev.*, 2001, vol. 222, p. 155.
5. Barnett, S.A. and Champness, N.R., *Coord. Chem. Rev.*, 2003, vol. 246, p. 145.
6. Batten, S.R. and Murray, K.S., *Coord. Chem. Rev.*, 2003, vol. 246, p. 103.
7. Kondo, M., Yoshitomi, T., Matsuzaka, H., et al., *Angew. Chem., Int. Ed. Engl.*, 1997, vol. 36, p. 1725.
8. Yaghi, O.M., *J. Am. Chem. Soc.*, 1998, vol. 123, p. 8571.
9. Chui, S.S., Lo, S.M., Charmant, J.P.H., et al., *Science*, 1999, vol. 283, p. 1148.
10. Li, H., Eddaoudi, M., O'Keeffe, M., and Yaghi, O.M., *Nature*, 1999, vol. 402, p. 276.
11. Férey, G., *Chem. Mater.*, 2001, vol. 13, p. 3084.
12. Kitagawa, S., Kitaura, R., and Noro, S., *Angew. Chem., Int. Ed. Engl.*, 2004, vol. 43, p. 2334.
13. Férey, G., *Chem. Soc. Rev.*, 2008, vol. 37, p. 191.
14. *Metal-Organic Frameworks, Design and Application,* MacGillivray, L.R., Ed., New York: Wiley, 2010, p. 349.
15. Yutkin, M.P., Dybtsev, D.N., and Fedin, V.P., *Usp. Khim.*, 2011, vol. 80, p. 1061.
16. Dybtsev, D.N., Chun, H., and Kim, K., *Angew. Chem., Int. Ed. Engl.*, 2004, vol. 43, p. 5033.
17. Chun, H., Dybtsev, D.N., Kim, H., and Kim, K., *Chem.-Eur. J.*, 2005, vol. 11, p. 3521.
18. Dybtsev, D.N., Sokolov, I.E., Peresypkina, E.V., and Fedin, V.P., *Izv. Akad. Nauk, Ser. Khim.*, 2007, p. 219.
19. Dybtsev, D.N., Yutkin, M.P., Peresypkina, E.V., et al., *Inorg. Chem.*, 2007, vol. 46, p. 6843.

20. Dybtsev, D.N., Yutkin, M.P., and Fedin, V.P., *Izv. Akad. Nauk, Ser. Khim.*, 2009, p. 2179.
21. Spek, A.L., *Acta Crystallogr., Sect. D: Biol. Crystallogr.*, 2009, vol. 65, p. 148.
22. Dybtsev, D.N., Nuzhdin, A.L., Chun, H., et al., *Angew. Chem., Int. Ed. Engl.*, 2006, vol. 45, p. 916.
23. Dybtsev, D.N., Yutkin, M.P., Samsonenko, D.G., et al., *Chem.-Eur. J.*, 2010, vol. 16, p. 10348.
24. Yutkin, M.P., Zavakhina, M.S., and Samsonenko, D.G., et al., *Izv. Akad. Nauk, Ser. Khim.*, 2010, p. 719.
25. Yutkin, M.P., Zavakhina, M.S., Samsonenko, D.G., et al., *Inorg. Chim. Acta*, 2013, vol. 394, p. 367.
26. Zavakhina, M.S., Samsonenko, D.G., Virovets, A.V., et al., *J. Solid State Chem.*, 2014, vol. 210, p. 125.
27. Vaidhyanathan, R., Bradshaw, D., Rebilly, J.-N., et al., *Angew. Chem., Int. Ed. Engl.*, 2006, vol. 45, p. 6495.
28. Perez Barrio, J., Rebilly, J.-N., Carter, B., et al., *Chem.-Eur. J.*, 2008, vol. 14, p. 4521.
29. Ingleson, M.J., Barrio, J.P., Bacsa, J., et al., *Chem. Commun.*, 2008, p. 1287.
30. Rood, J.A., Noll, B.C., and Henderson, K.W., *J. Solid State Chem.*, 2010, vol. 183, p. 270.
31. Kim, H., Samsonenko, D.G., Das, S., et al., *Chem. Asian J.*, 2009, vol. 4, p. 886.
32. Nuzhdin, A.L., Dybtsev, D.N., Bryliakov, K.P., et al., *J. Am. Chem. Soc.*, 2007, vol. 129, p. 12958.
33. Nuzhdin, A.L., Dybtsev, D.N., Fedin, V.P., and Bukhtiyarova, G.A., *Dalton Trans.*, 2009, p. 10481.
34. Suh, K., Yutkin, M.P., Dybtsev, D.N., et al., *Chem. Commun.*, 2012, vol. 48, p. 513.

Translated by E. Yablonskaya